Finite strain measurement from tagged cardiac MR images: Gabor filter approach

T. Manglik[1], L. Axel[1], V. M. Pai[1]

[1]Radiology, New York University, New York, NY, United States

Introduction

Myocardial tagging provides a potentially quantitative technique for assessing regional myocardial wall motion. In tagged cardiac MR images, the tag lines within the heart move and change shape as the heart contracts and relaxes through a heart cycle. This change in shape and position of the tag lines can be used to give detailed spatio-temporal information of the strain that develops within the heart. The underlying factors that influence the regional function of the heart, such as the contractile force that the heart generates, the pressure from the blood, tension in the heart muscle due to adjacent heart tissue, cannot be measured directly, but strain can be used to assess the local dynamics of the heart as it separates out the local deformation from the bulk motion. Methods for tagged image analysis commonly include segmenting the tags using a deformable model approach and require manual intervention and assistance during the segmentation process. Fourier based methods, such as HARP (1), are automated but have significant limitations. The aim of this study is to develop a new completely automated approach for computing strain and evaluate its performance on a numerical phantom.

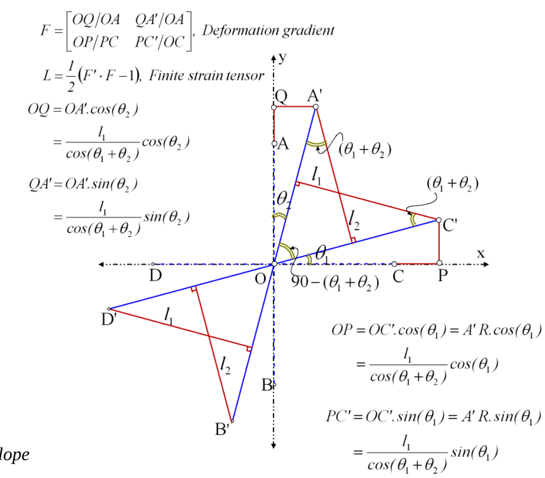

Figure2. Calculating deformation gradient and finite strain tensor from the spacing and orientation of the tags

Methods

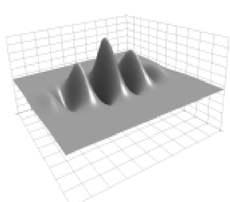

Figure1. Gabor filter

$h(x,y) = g(x',y').s(x,y)$

$g(x',y') =$ *Gaussian envelope*

$s(x,y) =$ *sinusoidal function*

$s(x,y) = sin(2\pi d/\lambda + \phi)$

$d = x cos\xi + y sin\xi$

$x' = +x cos\theta + y sin\theta$

$y' = -x sin\theta + y cos\theta$

$$g(x',y') = \frac{1}{2\pi\sigma_{x'}\sigma_{y'}} exp\frac{-\left((x'/\sigma_{x'})^2+(y'/\sigma_{y'})^2\right)}{2}$$

$\theta =$ *Orientation of Gaussian envelope*

$\sigma_x, \sigma_y =$ *Standard deviations of Gaussian envelope*

$\xi =$ *Orientation of sinusoid*

$\lambda =$ *Wavelength of sinusoid*

$(2\pi d/\lambda + \phi) =$ *Local phase of sinusoid*

$\phi =$ *Initial phase offset of sinusoid*

We use a bank of Gabor filters (2) to determine the local tag spacing and the orientation, for a set of initially perpendicular tags, at each pixel in image. Using these local tag spacings and tag orientations we determine the strain at that pixel in the image. A Gabor filter is a Gaussian modulated by a sinusoid (Fig. 1). It is defined as: As the heart changes shape, the tag spacing and orientation also change. Using a bank of Gabor filters with varying orientation and wavelength, we can find out which of these filters best matches the underlying tag pattern of the image. The best match filter has the highest response to the underlying image and its wavelength and orientation are the closest to the local tag spacing and orientation. In Fig. 2, AB and CD represent the initial tag spacing and orientation. After deformation, they change to A' B' and C'D' respectively. l, l_2, θ_1 and θ_2 (Fig. 2) are given by the wavelength and the orientation of the locally matching Gabor filter. The first principal strain and the second principal strain (usually principal shortening and principal thickening for a normal heart) are given by the eigen-vectors of the finite strain tensor. The method was verified on a numerically generated two-dimensional tagged phantom. The phantom underwent a set of six sequential displacements and deformations (three if them are shown in Fig. 3.) consisting of rotation and radial contraction with known strain values (Fig 4a.) The Gabor filter approach was used to compute strain of the deformed phantom in these images (Fig. 4b.)

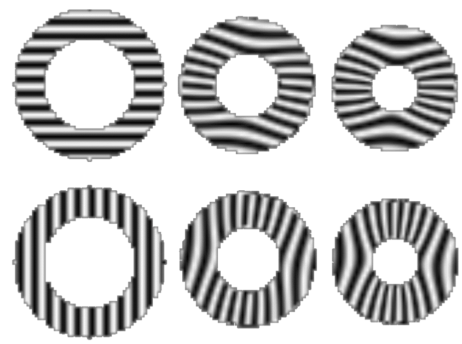

Figure3. Simulated Images 1,3,5 shown from deformation sequence of six images. The simulated motion consists of rotation and radial contraction.

Result

The mean absolute error between the magnitudes of the actual and computed principal thickening (Fig. 5a.) and shortening (Fig. 5b.) is shown in figure 5c. We also observe that most of the error (Fig. 4c.) is at the edges of the phantom. It is difficult to find the best locally matching Gabor filter on the boundary because the tag pattern is not continuous

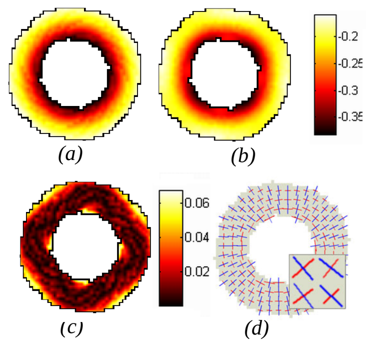

Figure 4. (a) Known principal thickening magnitude for the fourth image in the series of six images (b) Computed principal thickening magnitude. (c) Error in magnitude of principal thickening (d) Orientations of the principal thickening (red) and principal shortening (blue).A part of the image has been magnified in the right bottom corner.

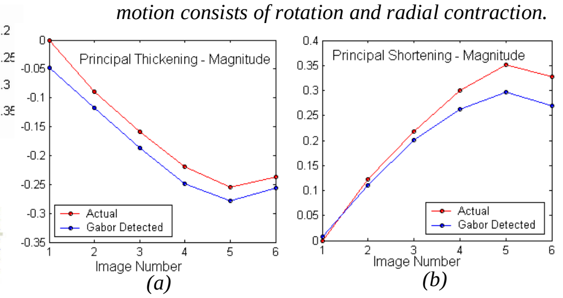

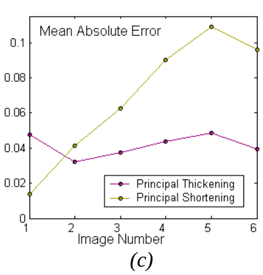

Figure5. The actual and the Gabor filter detected values of principal thickening (a) and shortening (b) for the series of six images. (c) The mean of the absolute error observed in the magnitudes of principal thickening and shortening.

Discussion

Gabor detection works at all places except the boundary. Hence the total error is proportional to how much surface the phantom has. For our computation, we did not track any tags, they were completely detected by the Gabor filter bank. Hence, the tag tracking was completely automated, although we did manually trace the boundary contours of the numerical phantom. We also observed that the performance of this method is extremely sensitive to the quality of the underlying image. Finally, note that for computation speed up, Gabor filter tag detection can be parallelized and distributed on multiple machines or processors.

References

1. Osman NF, Kerwin WS, McVeigh ER, Prince JL, MRM 1999 42:1048-1060
2. Gabor D, Journal of Institution of Electrical Engineers 1946 93,429-457